Ab initio Classical Trajectory Calculations: Application to Four-Centered HF Elimination from Vinyl Fluoride

Toshiyuki Takayanagi* and Atsushi Yokoyama

Advanced Science Research Center, Japan Atomic Energy Research Institute, Tokai-mura, Naka-gun, Ibaraki 319-11

(Received March 24, 1995)

Classical trajectories for four-centered HF elimination from vinyl fluoride have been calculated directly from *ab initio* molecular orbital results at the HF/3-21G level of theory, without the construction of an analytical potential energy function. The excess energy dependences of the product energy distributions and vector correlations were calculated. The calculated results were compared with available experimental data and qualitative agreements were obtained. However, in order to obtain quantitative agreements, trajectory analyses at a more accurate *ab initio* level of theory seem to be necessary.

The classical trajectory method is an important tool for understanding the dynamics of chemical reactions.[1] A large number of chemical reactions have been studied using this method.[2] However, such studies have been restricted to relatively simple systems such as A+BC→AB+C type reactions because the construction of the potential energy surface is relatively easy. In the traditional approach, analytical potential energy functions are frequently employed. The parameters used in the functions are determined so as to reproduce the experimental data and/or potential energies obtained by *ab initio* molecular orbital calculations. The application of such a procedure to general polyatomic reaction systems having four atoms or more is rather difficult because polyatomic reaction systems have various product channels and many degrees of freedom. Many classical trajectory studies using the analytical functions have been carried out.[3—8] However, in general, the analytical functions employed in a study cannot be applied to other polyatomic reaction systems since such functions are developed so as to reproduce the potential characteristics for a specific product channel.

Another method for calculating classical trajectories is to use *ab initio* computational results without construction of analytical potential functions. This method has rapidly become useful because of recent advances in computational speed and improvements over *ab initio* molecular orbital programs. In fact, as compared with the construction of analytical potential functions from ordinary grid calculations of potential energies by *ab initio* methods, the direct use of *ab initio* results in trajectory calculations is an economical method, especially for systems having more than three atoms. For example, in the case of a six-atom system, ten grid points in each internal coordinate result in a total of 10^{12} grid points because the system has twelve internal coordinates. On the other hand, the trajectory calculations require about 10^3—10^4 potential energies and energy derivatives for producing one trajectory. Thus, a total of 10^6—10^7 points of energy and energy derivatives are needed if we try to calculate 1000 trajectories. In addition, the energy derivatives can be calculated in a reasonable CPU time using analytical gradient techniques in *ab initio* computational software.

Recently, Helgaker and his co-workers[9,10] have applied *ab initio* trajectory calculations to H_2 eliminations from H_3 and CH_2OH^+. In order to save computational time, they solved the classical equations of motion on a local quadratic potential surface which is obtained from the first and second derivative calculations. Very recently, Chen et al.[11] have calculated the classical trajectories for the $H_2CO \rightarrow H_2+CO$ dissociation directly from *ab initio* methods. They have employed local fifth-order polynomial surfaces fitted to the energies, first and second derivatives. They have obtained several hundreds of trajectories to calculate the energy distributions of the products.

In this paper, we apply the *ab initio* classical trajectory method to four-centered hydrogen fluoride (HF) elimination from vinyl fluoride. The unimolecular reaction of vinyl fluoride is one of the simplest polyatomic systems and has been studied experimentally and theoretically for quite some time. For example, the vibrational distribution of HF produced in the infrared multiphoton dissociation (IRMPD) of vinyl fluoride has been measured by Quick and Wittig.[12] Very recently, Sato et al.[13] have measured the translational energy distributions of the fragments produced in the photodissoci-

ation at 157 nm. From a theoretical point of view, Kato and Morokuma[14] have carried out extensive *ab initio* molecular orbital calculations for the unimolecular reactions of vinyl fluoride and obtained characteristics of the potential surface for HF elimination. Thus, critical comparisons with other studies are possible. Without the use of any fitting procedures for obtaining a potential energy surface, the classical equations of motion are numerically solved using only the *ab initio* energies and first derivatives. In order to calculate the classical trajectories at a reasonable cost, we have modified the HONDO *ab initio* computational program.[15]

Computational Method

As mentioned in the Introduction, the classical equations of motion can be solved using *ab initio* energies and first energy derivatives directly. The *ab initio* computational code was modified in order to reduce the computational time. The *ab initio* code employed was the HONDO version 7 system[15] and was extensively modified so as to save all the files including molecular integrals into computer memory.

The classical equations of motion were solved numerically using a standard fifth-order predictor–corrector method. A trajectory was terminated when the distance between the two fragments, HF and acetylene, was greater than 12 bohr. The step size employed was 7×10^{-17} s, which was determined so as to conserve the total energy within 99.99%. The *ab initio* calculations were carried out at the Hartree–Fock (HF) level of theory with a 3—21 G basis set. Of course, this level of theory may be inadequate for quantitative comparisons with experimental data since the Hartree–Fock theory does not include an electron correlation effect. Nevertheless, we believe that this method is valuable as an early stage of this type of investigation because several hundreds of trajectories can be calculated for a reasonable cost. A typical CPU time for producing one trajectory was about 120 min on an IBM RS/6000 590 workstation.

The initial conditions were selected using an orthant-like sampling method.[6—8] Each trajectory was started at the molecular geometry around the saddle point. The absolute values of the momenta were determined randomly in the interval (0, P_{max}), where P_{max} is the absolute value of the momentum in the case when all the atoms have the same kinetic energy. The three orientation angles of each momentum vector were also determined randomly. The spurious center-of-mass momentum and the total angular momentum were then subtracted. In general, the randomness for the selection of the initial conditions may affect the results of the trajectory calculations. However, as is mentioned in the following section, an approximately linear relationship exists between the average values for the product energies and the excess energy which is the difference between total energy and a classical barrier height. This behavior tentatively suggests the selection of the initial conditions employed in the present calculation is reasonable.

The calculations were carried out for three excess energies. The number of total reactive trajectories calculated was 108 for 1 kcal mol^{-1} of excess energy, 228 for 10 kcal mol^{-1}, and 321 for 50 kcal mol^{-1}.

Results and Discussion

A. Characteristics of the Potential Energy Surface. Figure 1 shows the potential energy profile along the intrinsic reaction coordinate (IRC) at the HF/3—21 G level of theory. Figure 1 also shows the molecular geometry at the saddle point. The optimized geometry obtained is essentially the same structure as that calculated by Kato and Morokuma[14] at the HF/4—31 G level of theory although their calculations give slightly larger distances for the C–F and H–F bonds and a shorter value for the C–H bond. These behaviors indicate that the potential energy surface at the HF/4—31 G level of theory has an early barrier, while the potential at the HF/3—21 G level of theory has a late barrier. The classical barrier height and endothermicity were calculated to be 92.0 and 40.4 kcal mol^{-1}, respectively. Kato and Morokuma[14] have also estimated the barrier height and the exothermicity by using a more accurate method including configuration interactions with a larger 6—31 G** basis set. They obtained 86.8 kcal mol^{-1} for the barrier height and 30.3 kcal mol^{-1} for the endothermicity. On the other hand, the experimental activation energy has been estimated to be 70—80 kcal mol^{-1}[16,17] and the experimental endothermicity has been reported to be about 18 kcal mol^{-1}.[18,19] The values calculated in the present study are larger than the experimental ones as well as the theoretical

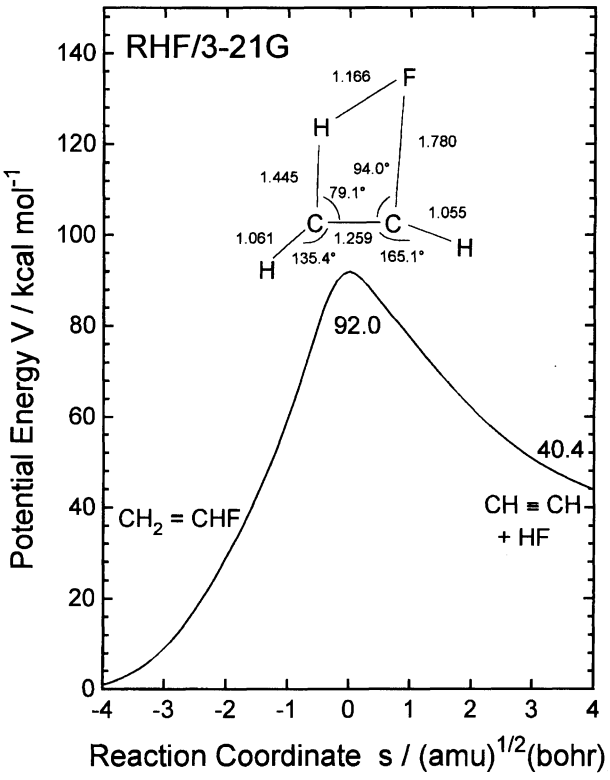

Fig. 1. Potential energy profile along the intrinsic reaction coordinate (IRC). Unit of IRC is given in (amu)$^{1/2}$(bohr).

ones obtained by Kato and Morokuma, but the calculated exit barrier height, which corresponds to the potential energy difference between the saddle point and the asymptotic product channel, is comparable to the experimental value. This is encouraging since we can compare the present computational results with the experimental results quantitatively.

B. Details of a Sample Trajectory. A typical reactive trajectory for HF elimination from vinyl fluoride is plotted in Fig. 2. The excess energy used is 1 kcal mol^{-1}. The motions of the hydrogen atoms are quite noticeable because of their light mass. It is also found that both the C–H stretching and C–C–H bending vibrations are strongly excited in the product acetylene molecule. This behavior can be easily predicted from the molecular geometry at the saddle point; one C–C–H bending angle is deviated from 180° as shown in Fig. 1. In addition, the C–C stretching vibration is found to be slightly excited. The trajectory shows that the F atom in the HF molecule and the two C atoms in the acetylene molecule move in nearly opposite directions. This means that the potential energy surface calculated at the HF/3—21 G level of theory has a repulsive character in the exit channel. Therefore, it is expected that a large

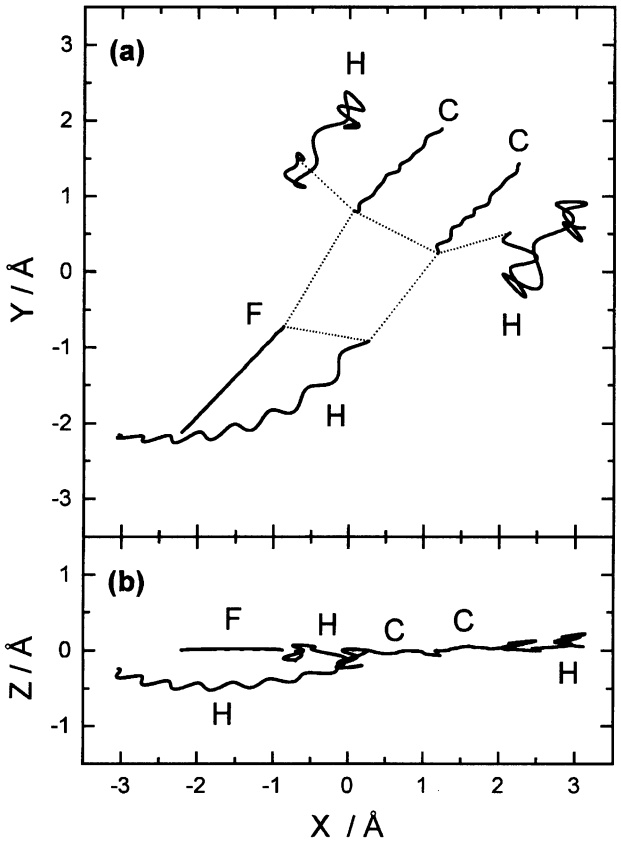

Fig. 2. A typical reactive trajectory for HF elimination from vinyl fluoride plotted in Cartesian coordinates. The excess energy is 1 kcal mol^{-1}. Dotted lines indicate the molecular structure at the saddle point.

amount of the exit barrier energy is mainly partitioned into the relative translational energy. This prediction is also supported by the fact that the reaction completes within a very short time (typically 20—30 fs).

C. Product Energy Distributions. Figure 3 shows the distributions of the relative translational energy, the vibrational energy of the product HF, the rotational energy of the product HF, and the internal energy of the product C_2H_2 at three values of excess energies E_x=1, 10, and 50 kcal mol^{-1}. In the calculations of the HF vibrational and rotational energy distributions, coupling between the vibration and rotation was ignored. The internal energy of C_2H_2 includes both the vibrational and rotational energies.

As for the relative translational energy, it is noted that higher excess energy gives a broader distribution, while the change in the peak values of the distributions is not so large. The distributions are approximately Gaussian-shaped with peak values of 40.6, 40.7, and 44.8 kcal mol^{-1} and full widths at half maxima of 2.5, 8.0, and 16.9 kcal mol^{-1} at excess energies of 1, 10, and 50 kcal mol^{-1}, respectively. It was found that a large amount of the total available energy is partitioned into the relative translational energy. The fractions were calculated to be 77, 66, and 44% at excess energies of 1, 10, and 50 kcal mol^{-1}, respectively. These large fractions are simply explained by the repulsive nature of the potential energy surface employed in the present calculations, as mentioned before.

The vibrational distributions of the product HF show a non-statistical behavior and a small enhancement in comparison with a statistical distribution. The average energies were calculated to be 1.9, 4.0, and 8.8 kcal mol^{-1} at excess energies of 1, 10, and 50 kcal mol^{-1}, respectively.

The energy partitioned into the HF rotation was found to be very small. The average energies are 0.1, 0.5, and 4.0 kcal mol^{-1} at excess energies of 1, 10 and 50 kcal mol^{-1}, respectively. The rotational energy distributions were found to be well-represented by Boltzmann distributions. The resulting rotational temperatures are 45, 270, and 1400 K at excess energies of 1, 10, and 50 kcal mol^{-1}, respectively.

In order to analyze more precisely the contribution of the excess energy and the exit barrier height to the product energies, the average of each type of energy is plotted as a function of excess energy E_x in Fig. 4. Figure 4 shows that each type of product energy E_i follows a linear relation as:

$$E_i = E_i^0 + a_i E_x. \quad (1)$$

Here, E_i^0 means the energy partitioned into a different type of product energy at zero excess energy and is determined from the nature of the potential energy surface. On the other hand, a_i is the fraction of excess energy partitioned into the different type of product en-

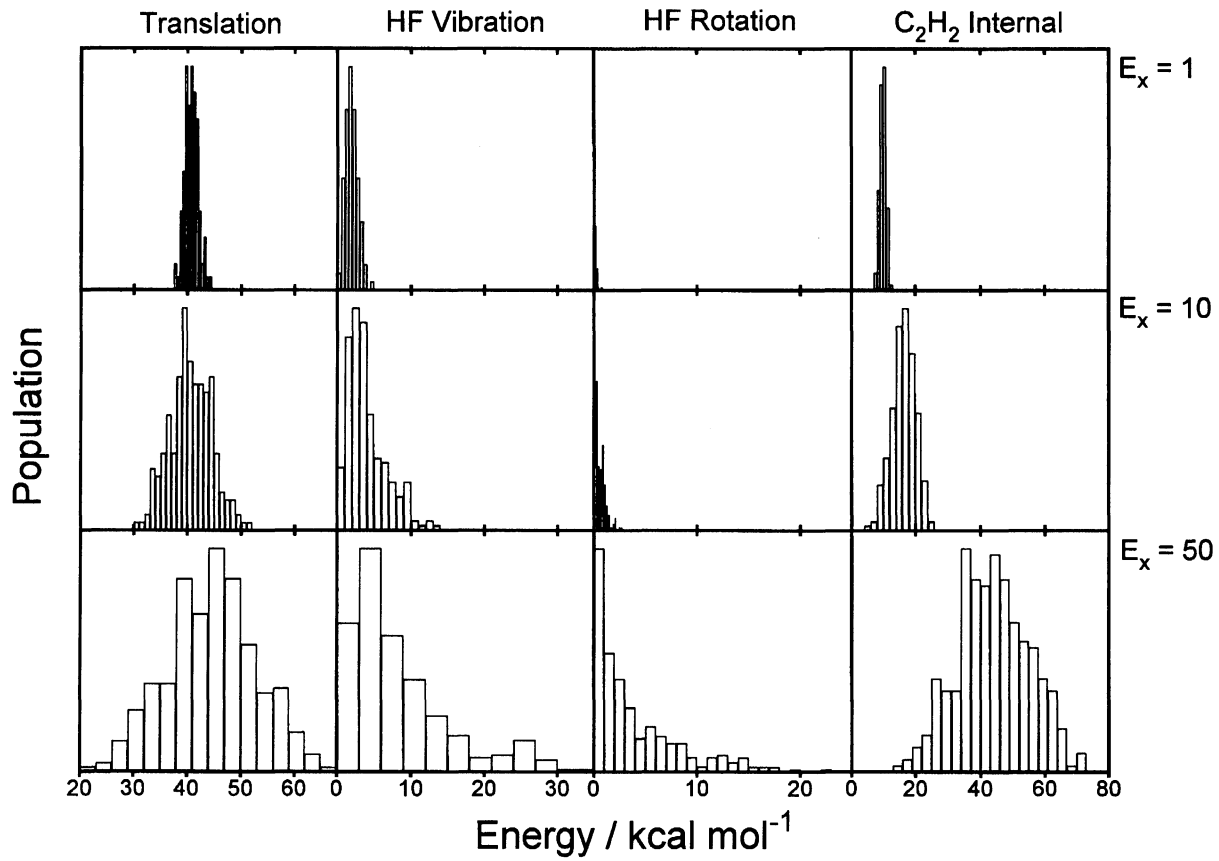

Fig. 3. Relative translational energy distributions, HF vibrational energy distributions, HF rotational energy distributions, and C_2H_2 internal energy distributions at three values of excess energies E_x.

ergy. E_i^0 and a_i obtained by a least-squares method are summarized in Table 1. Table 1 also includes the values of a_i which are statistically predicted from the number of degrees of freedom. For the relative translational energy and the HF rotational energy, the calculated values of a_i are comparable to the values predicted statistically. For the HF vibrational energy, however, the value of a_i is larger than the statistical value. Thus, the opposite trend results in the internal energy of C_2H_2. This behavior suggests that coupling between the HF vibrational modes and the reaction coordinate exists in the exit channel of the potential energy surface.

Kato and Morokuma[14] have reported that the energy distributed in the HF vibration is 11.5 kcal mol^{-1} from an IRC analysis. Our trajectory calculations give about 2 kcal mol^{-1} for the HF vibrational energy at zero excess energy. This difference can qualitatively be explained by the difference in the characteristics of the potential energy surfaces. As mentioned in the previous section, the potential surface at the HF/4—31 G level has an early barrier, while the potential at the HF/3—21 G level has a late barrier. However, in order to obtain a more quantitative conclusion, trajectory calculations at the HF/4—31 G level of theory should be carried out.

Table 1. Parameters of the Linear Variation of Each Type of Energy with the Excess Energy

Type of energy	E_i^0/kcal mol^{-1}	a_i	a_i(stat.)[a]
Translation	40.16±0.43	0.09±0.01	0.08
HF Vibration	2.16±0.50	0.14±0.02	0.08
HF Rotation	−0.11±0.17	0.09±0.01	0.08
C_2H_2 Internal	9.39±0.10	0.69±0.00	0.75

a) a_i (stat.) means the fractions which are predicted statistically from the degrees of freedom.

D. Vector Correlations. Details of the photodissociation dynamics can be obtained from not only the product energy distributions, but also the vector correlations. Figure 5 shows ***J*–*v*** correlations between the rotational angular momentum vectors $\boldsymbol{J}$ of HF and C_2H_2 and the relative velocity vector $\boldsymbol{v}$ for the three excess energies. Both the vector correlations exhibit maxima at around 90°. This is explained by the fact that the molecular structure at the saddle point is planar. The velocity vector must be parallel to this plane, while the rotational angular momentum vectors must be perpendicular to the plane. In addition, since the reaction occurs within a very short time, the directions of the rotational angular momentum vectors and velocity vector may be determined in an early stage of the reaction. It is also noted that the vector correlations do not depend on the excess energy. This suggests that the experimental measurements of the vector correlations give purely dynamical information about HF elimination from vinyl

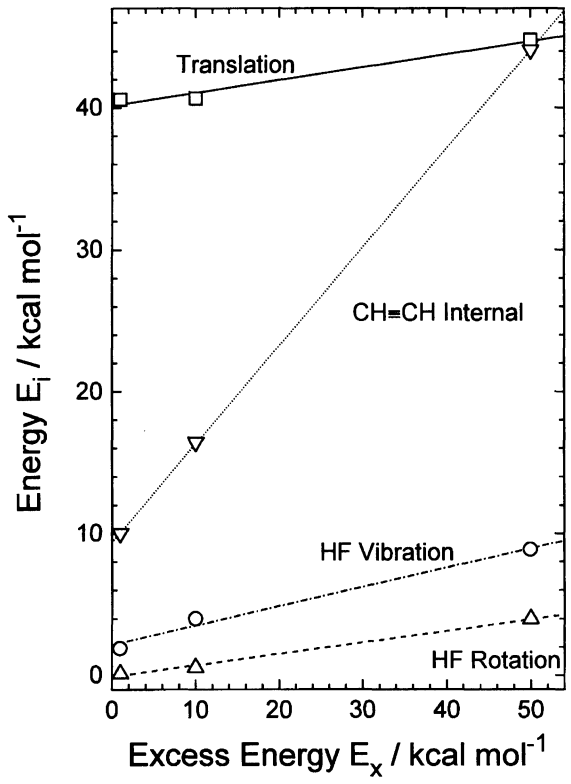

Fig. 4. Dependence of each type of product energy on the excess energy.

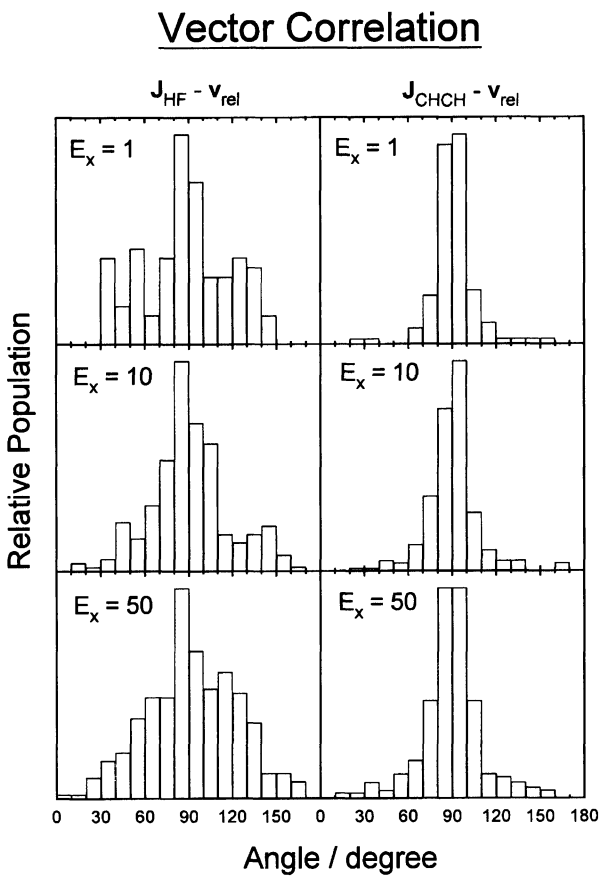

Fig. 5. Plots in the left column indicate the vector correlations between the rotational angular momentum vector of the product HF (J_{HF}) and the relative velocity vector (v_{rel}) for the three values of excess energies E_x. Plots in the right column are for the vector correlations between the rotational angular momentum vector of the product acetylene (J_{CHCH}) and the relative translational vector.

fluoride.

Figure 6 shows the vector correlations between the two rotational angular momentum vectors and the relative orbital angular momentum vector $\boldsymbol{L}$. The distributions show peaks at around 180° indicating that the two vectors have opposite directions. An explanation similar to the case for the $\boldsymbol{J}$–$\boldsymbol{v}$ correlations is also possible for the present case. In addition, the sharp distributions observed are due to the initial condition in which the total angular momentum is zero.

Figure 7 shows the $\boldsymbol{J}$–$\boldsymbol{J}$ vector correlations between the rotational angular momentum vectors of HF and C_2H_2. The $\boldsymbol{J}$–$\boldsymbol{J}$ correlation gives information about the exit dihedral angle between the two fragments. The distributions calculated show somewhat broad behavior for all excess energies although the populations $<90°$ are slightly large.

E. Comparisons of the Trajectory Results with Experimental Data. Before comparing the trajectory results with experimental data, we will discuss the accuracy of the asymptotic potential energy surfaces calculated at the HF/3—21 G level of theory. For the product HF molecule, we compared the *ab initio* potential curve with an experimental Morse curve. It was found that the *ab initio* potential curve becomes more inaccurate as the potential energy becomes larger. This can easily be predicted because it is generally accepted that the Restricted-Hartree–Fock theory does not give an accurate dissociation limit. This behavior is also the case for the potential surface of acetylene. Then, the trajectory calculations may overestimate the asymptotic potential energy especially for large excess energies. However, the errors were found to be within 2 kcal mol^{-1} for the trajectory calculations at an excess energy of 50 kcal mol^{-1}.

The vibrational state distribution of HF produced in IRMPD of vinylflouride has been reported by Quick and Wittig.[12] They have estimated that the experimental excess energy lies in the range of 20—35 kcal mol^{-1}. The experimental results and the present trajectory results are summarized in Table 2. Both the experimental and theoretical distributions show that the relative population decreases with an increase in the vibrational level although the population of HF ($v=0$) has not been measured in the experiment. However, the experimental result gives a slightly hotter distribution than the theoretical one even at an excess energy of 50 kcal mol^{-1}.

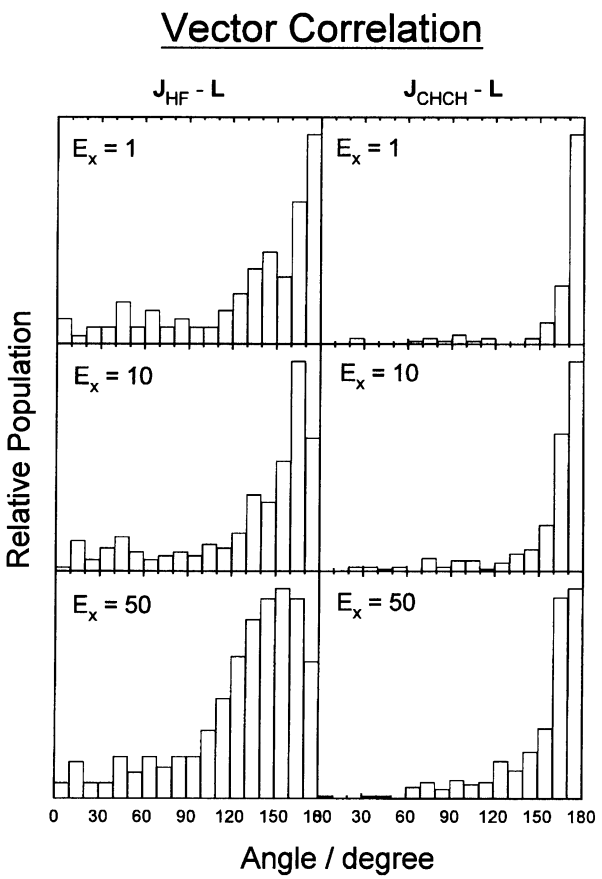

Fig. 6. Plots in the left column indicate the vector correlations between the rotational angular momentum vector of the product HF (J_{HF}) and the orbital angular momentum vector (L) for the three values of excess energies E_x. Plots in the right column are for the vector correlations between the rotational angular momentum vector of the product acetylene (J_{CHCH}) and the orbital angular momentum vector.

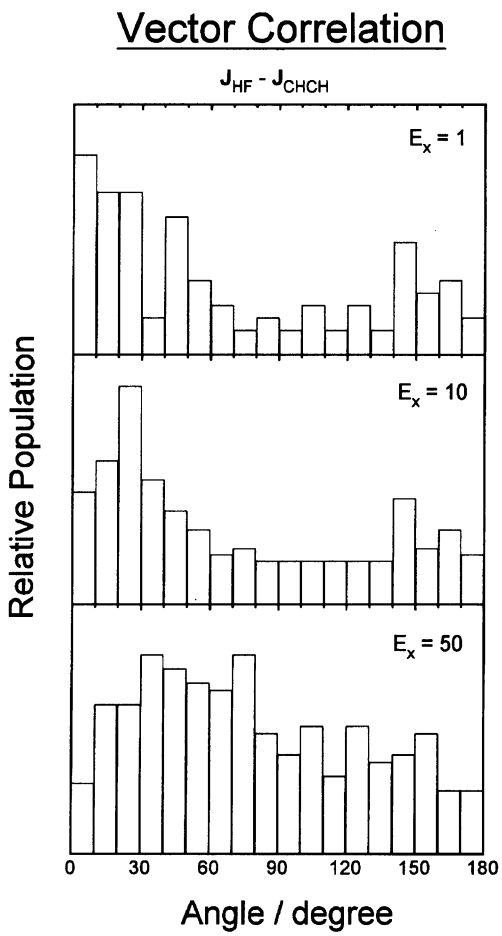

Fig. 7. The vector correlations between the rotational angular momentum vector of HF (J_{HF}) and the rotational angular momentum vector of acetylene (J_{CHCH}) for the three values of excess energies E_x.

Table 2. Comparison of the Vibrational State Distributions of HF(v) Produced in the Photodissociation of Vinyl Fluoride

E_x/kcal mol^{-1}	v=0	v=1	v=2	v=3	v=4
Experiment[a]					
20—35	—	1.0	0.55	0.15	< 0.05
Trajectory[b]					
1	100	0	0	0	0
10	79	21	0	0	0
50	47	41	10	1	1

a) The experimental distributions are normalized at the population of HF (v=1) because the population of HF (v=0) has not been measured. b) The vibrational distributions calculated by the trajectory method are expressed in percentage.

Very recently, Sato et al.[13] have measured the relative translational energy of HF elimination from vinyl fluoride by using a time-of-flight technique. They have concluded from the extrapolation to zero excess energy that about 64% of the exit barrier height is partitioned into the relative translational energy. On the other hand, the present trajectory calculations give 40.2 kcal mol^{-1} as the relative translational energy at zero excess energy, corresponding to 78% of the exit barrier height. Thus, the experimental value is smaller than the theoretical one. However, both the experimental data and the present trajectory calculations indicate that a large amount of the exit barrier energy is partitioned into the relative translational energy.

Concluding Remarks

In this paper we have studied the dynamics of HF elimination from vinyl fluoride by using a classical trajectory method in which the potential energies and energy derivatives are calculated directly from the *ab initio* molecular orbital method without constructing an analytic potential function. The *ab initio* calculations have been carried out at the HF/3—21 G level of theory. The product energy distributions including the relative translational energy, the vibrational and rotational energies of the product HF, and the internal energy of

the product C_2H_2 have been presented. Vector correlations have also been calculated and were found to give important information for understanding the reaction dynamics. Qualitative agreements with available experimental data have been obtained for the product energy distributions. In order to obtain more quantitative agreements with the experimental data, it will be necessary to carry out trajectory calculations at more accurate levels of *ab initio* methods including electron correlation effects. Such a calculation is possible if a large CPU time is available. Consequently, the classical trajectory method with the direct use of *ab initio* results may be applied to various polyatomic reaction systems in the near future because of rapid advances in computer speed.

References

1) R. D. Levine and R. B. Bernstein, "Molecular Reaction Dynamics and Chemical Reactivity," Oxford University Press, New York (1987).

2) D. G. Truhlar and J. T. Muckerman, "Atom–Molecule Collision Theory, a Guide for the Experimentalists," ed by R. B. Bernstein, Plenum Press, London (1979), p. 505.

3) W. L. Hase, "Potential Energy Surfaces and Dynamical Calculations," ed by D. G. Truhlar, Plenum Press, New York (1980), p. 1.

4) R. N. Porter and L.M. Raff, "Dynamics of Molecular Collisions," ed by W. H. Miller, Plenum Press, New York (1976), p. 1.

5) D. L. Bunker, *Methods Comput. Phys.*, **10**, 287 (1971).

6) R. M. Benito and J. Santamaria, *J. Phys. Chem.*, **92**, 5028 (1988).

7) R. M. Benito and J. Santamaria, *Chem. Phys. Lett.*, **109**, 478 (1984).

8) R. M. Benito and J. Santamaria, *Chem. Phys. Lett.*, **155**, 391 (1989).

9) T. Helgaker, E. Uggerud, and H. J. A. Jensen, *Chem. Phys. Lett.*, **173**, 145 (1990).

10) E. Uggerud and T. Helgaker, *J. Am. Chem. Soc.*, **114**, 4265 (1992).

11) W. Chen, W. L. Hase, and H. B. Schlegel, *Chem. Phys. Lett.*, **228**, 436 (1994).

12) C. R. Quick, Jr., and C. Wittig, *J. Chem. Phys.*, **72**, 1694 (1980).

13) K. Sato, T. Takayanagi, G. Fujisawa, and A. Yokoyama, to be published.

14) S. Kato and K. Morokuma, *J. Chem. Phys.*, **74**, 6285 (1981).

15) M. Dupuis, J. D. Watts, H. O. Villar, and G. J. B. Hurst, "HONDO Version 7," *Comput. Phys. Commun.*, **52**, 415 (1989).

16) P. Cadman and W. J. Engelbrecht, *J. Chem. Soc., Chem. Commun.*, **1970**, 203.

17) J. M. Simmie, W. J. Quiring, and E. Tschuikow-Roux, *J. Phys. Chem.*, **74**, 992 (1970).

18) V. P. Kolesov and T. S. Papina, *Zh. Fiz. Khim.*, **44**, 1101 (1970).

19) "JANAF Thermochemical Tables," Nat. Stand. Ref. Data Ser., Nat. Bur. Stand. 37, U. S. Government Printing Office, Washington, D. C. (1972).